Secretory Expression of Cyclohexanone Monooxygenase by Methylotrophic Yeast for Efficient Omeprazole Sulfide Bio-oxidation

Ya-Jing Li
East China University of Science and Technology
Yu-Cong Zheng
East China University of Science and Technology https://orcid.org/0000-0001-8509-3127
Qiang Geng
East China University of Science and Technology
Feng Liu
East China University of Science and Technology
Zhi-Jun Zhang
East China University of Science and Technology
Jian-He Xu
East China University of Science and Technology
Hui-Lei Yu (huileiyu@ecust.edu.cn)
East China University of Science and Technology https://orcid.org/0000-0002-1925-3679

Research Article

Keywords: cyclohexanone monooxygenase, omeprazole sulfoxide, Pichia pastoris, secretory expression, asymmetric oxidation

Posted Date: June 22nd, 2021

DOI: https://doi.org/10.21203/rs.3.rs-600789/v1

Abstract

Prochiral pyrmetazole can be asymmetrically oxidized into (*S*)-omeprazole, a proton pump inhibitor that is used to treat gastroesophageal reflux, by an engineered cyclohexanone monooxygenase ($CHMO_{Acineto}$-Mut) that has high stereoselectivity. $CHMO_{Acineto}$-Mut is produced by heterologous expression in *Escherichia coli*, where it is expressed intracellularly. Thus, isolating this useful biocatalyst requires tedious cell disruption and subsequent purification, which hinders its use for industrial purposes. Here, we report the extracellular production of $CHMO_{Acineto}$-Mut by a methylotrophic yeast, *Pichia pastoris,* for the first time. The recombinant $CHMO_{Acineto}$-Mut expressed by *P. pastoris* showed a higher flavin occupation rate than that produced by *E. coli*, and this was accompanied by a 3.2-fold increase in catalytic efficiency. At a cell density of 150 g/L cell dry weight, we achieved a recombinant $CHMO_{Acineto}$-Mut production rate of 1,700 U/L, representing approximately 85% of the total protein secreted into the fermentation broth. By directly employing the pH adjusted supernatant as a biocatalyst, we were able to almost completely transform 10 g/L of pyrmetazole into the corresponding (*S*)-sulfoxide, with >99% enantiomeric excess.

Introduction

Bayer–Villiger monooxygenase (BVMO) is a flavin-dependent enzyme that catalyzes the regioselective Bayer–Villiger oxidation of ketones to the corresponding esters or lactones [Fürst et al. 2019; Romero et al. 2018; de Gonzalo et al. 2010]. BVMOs show broad substrate acceptance of aliphatic ketones [Forney et al. 1969; Yu et al. 2018; Fiorentini et al. 2017] and aromatic extended ketones [van Beek et al. 2012; Fraaije et al. 2005], and also catalyze other oxidation reactions, including hydroxylation [Ferroni et al. 2017; Bisagni et al. 2014], epoxidation [Colonna et al. 2002; Rial et al. 2008], and sulfoxidation [Branchaud et al. 1985; de Gonzalo et al. 2017]. As BVMO catalysis reactions have high enantio-, regio-, and chemo-selectivity, involve a “green” oxidant (oxygen), and utilize the easily recycled NAD(P)H [Mordhorst et al. 2020] as the electronic donor, BVMOs are attracting increasing attention for their potential utility in environmentally benign bio-oxidation processes.

Cyclohexanone monooxygenase (CHMO), one of the most well-characterized type I BVMOs [de Gonzalo et al. 2010], was first identified in *Acinetobacter* sp. strain NCIMB 9871 ($CHMO_{Acineto}$) [Donoghue et al. 1976]. Native $CHMO_{Acineto}$ has a strong preference of Bayer–Villiger oxidation of tetratomic to hexatomic ring ketones [Light et al. 1982]. In a recent study, $CHMO_{Acineto}$ was subjected to several rounds of directed evolution, resulting in the generation of a mutant ($CHMO_{Acineto}$-Mut) with a significant capacity for asymmetric oxidation of pyrmetazole [Bong et al. 2018]. This mutant enzyme is used to produce esomeprazole ((*S*)-omeprazole), a popular drug for the clinical treatment of gastroesophageal reflux [Carreno et al. 1995; Matsui et al. 2014]. Later studies used genomic mining [Liu et al. 2021; Zhang et al. 2018] or directed evolution to generate several other BVMOs that are capable of transforming sulfides with a “prazole” scaffold [Zhang et al. 2019; Ren et al. 2020; Zhao et al. 2021].

A competitive industrial enzymatic oxidation process always requires a robust biocatalyst, which should be readily available in terms of quantity and have a sufficient activity level. However, both the engineered CHMOs and other native BVMOs are still limited by relatively low activity toward bulky pyrmetazole derivatives. Furthermore, an additional purification step is needed to isolate $CHMO_{Acineto}$-Mut, which is produced intracellularly in *Escherichia coli* [Bong et al. 2018]. Another issue that should be addressed is the existence of endotoxins in *E. coli* systems, which would bring contamination and affect the quality of the target pharmarco sulfoxides [Hasegawa et al. 1999; Yang et al. 2008] that it is used to manufacture. Although intracellular expression of CHMOs in generally recognized as safe (GRAS) hosts such as *Saccharomyces cerevisiae* has been shown to be feasible [Chen et al. 1999; Stewart et al. 1996], to date, extracellular production of this enzyme family has not been reported. A safe and efficient heterologous extracellular expression system for CHMO that eliminates the need for cell-breaking and purification steps is therefore needed to achieve large-scale production of high-quality enzymes for industrial applications.

The methylotrophic yeast *Pichia pastoris* (*Komagataella phaffii*) is an established, Food and drug administration (FDA) approved, safe and highly competitive extracellular expression host that secretes large amounts of heterologous proteins and only low amounts of endogenous proteins [Karbalaei et al. 2020; Cereghino et al. 2000]. Here, we report for the first time extracellular expression of $CHMO_{Acineto}$-Mut by *P. pastoris*. The $CHMO_{Acineto}$-Mut–containing culture broth was used directly to achieve efficient enzymatic synthesis of (*S*)-omeprazole.

Experimental

Chemicals and enzymes

All sulfides, sulfoxides, and sulfones were kindly provided by Aosaikang Pharmaceutical Co., (Nanjing, China). Primer STAR HS and restriction enzymes (*Eco*R I, and *Not* I), and T_4 DNA ligase were purchased from Takara Bio-technology Co., (Dalian, China). Primers were synthesized by Generay Biotech Co., (Shanghai, China). Unless otherwise stated, all other chemicals and reagents used in this work were obtained commercially and were of reagent grade.

Strains, plasmids and media

Strains of *E. coli* BL21 (DE3) and *E. coli* DH5α were purchased from TransGen Biotech Co., Ltd (Beijing, China). *E. coli* DH5α was used for the construction of recombinant plasmids. The *E. coli* strain BL21 (DE3) and the plasmid pET-28a(+) were used for protein expression. *Pichia pastoris* X33 and pPICZαA/pGAPZαA were used for the secretory expression of $CHMO_{Acineto}$-Mut.

Luria broth medium (LB, 1% tryptone, 0.5% yeast extract, 1% NaCl), LBK (supplied with kanamycin), Yeast extract–peptone dextrose medium (YPD, 1% yeast extract, 2% peptone and glucose), YPDZ (supplied with zeocin), buffered glycerol–complex medium (BMGY, 1% yeast extract, 2% peptone, 100 mM potassium

phosphate (pH 6.0), 0.4 ppm of biotin, 1.34% yeast nitrogen base without amino acids, 1% glycerol), buffered methanol–complex medium (BMMY, 1% yeast extract, 2% peptone, 200 mM potassium phosphate (pH 6.0), 0.4 ppm of biotin, 1.34% yeast nitrogen base, 1% methanol), fermentation basal salts medium (BSM: phosphoric acid (85%, 21 mL/L), $CaSO_4$ (0.9 g/L), K_2SO_4 (14.3 g/L), $MgSO_4$ (6.0 g/L), potassium hydroxide (3.3 g/L) and glycerol (40 g/L)), after autoclaved, 8 mL/L of PTM1 solution was supplied and the pH of the medium was adjusted to 6.0 by ammonia, PTM1 trace salts solution: biotin (0.2 g/L), $CuSO_4 \cdot 5H_2O$ (6.0 g/L), KI (0.09 g/L), $MnSO_4 \cdot H_2O$ (3 g/L), $Na_2MoO_4 \cdot 2H_2O$ (0.2 g/L), H_3BO_3 (0.02 g/L), $CoCl_2 \cdot 6H_2O$ (0.9 g/L), $ZnSO_4 \cdot 7H_2O$ (42.2 g/L), concentrated H_2SO_4 (5 mL/L), $FeSO_4 \cdot 7H_2O$ (65 g/L). Glycerol feeding medium: 50% glycerol supplied with 12 mL/L of PTM1 trace salts solution. Methanol feeding medium: neat methanol supplied with 12 mL/L PTM1 trace salts solution. Bacterial fermentation medium: 0.5% peptone, 0.5 yeast extract, 0.5% glycerol, 0.9% $Na_2HPO_4 \cdot 12H_2O$, 0.07% Na_2SO_4, 0.34% KH_2PO_4, 0.025% $MgSO_4$, 0.27% NH_4Cl. Complex feeding medium: 6% peptone, 6% yeast extract, 25% glycerol.

Expression and purification of $CHMO_{Acineto}$-Mut expressed by *E. coli* BL21 (DE3)

The sequence of the engineered $CHMO_{Acineto}$-Mut gene was designed with a histidine tag at the *N*-terminal, synthesized and subsequently cloned into pET-28a(+) by Genscript Biotech (Nanjing) Co., Ltd (Nanjing, China). Transformants were cultured for 12 h in test tubes containing 4 mL of LB medium with 50 μg/mL kanamycin at 37°C and 180 rpm, and then 1 mL of the culture was inoculated into 100 mL of fresh LB medium containing 50 μg/mL kanamycin. After cultivation at 37°C, 180 rpm for 2.5 h, isopropyl-*β-D*-thiogalactoside (IPTG) and vitamin B solutions were added to a final concentration of 0.2 mM, and 50 mg /L, respectively. Induction was started when the optical density (OD_{600}) of the *E. coli* cells arrived at 0.6 to 0.8, and further proceeded for 20 h at 16°C, 180 rpm. The induced cells were harvested by centrifugation and lysed by ultra-sonication, and the cell lysate was centrifuged at 10,000×*g* and 4°C for 30 min. The supernatant was then loaded onto a HisTrap HP (GE, USA) column which was pre-equilibrated with Ni-NTA buffer A (potassium phosphate, 20 mM, pH 7.4; sodium chloride, 500 mM; 2-mercaptoethanol, 5 mM). Samples were eluted by gradient imidazole by employing Ni-NTA buffer B (Ni-NTA buffer A containing 500 mM of imidazole). Elution fractions which contained highly pure $CHMO_{Acineto}$-Mut were pooled, desalted with Ni-NTA buffer C (potassium phosphate, 20 mM, pH 7.4; sodium chloride, 150 mM; dithiothreitol, 1 mM) and flash frozen in liquid nitrogen, stored at −80°C for further analysis.

Cloning and expression of the $CHMO_{Acineto}$-Mut gene in *P. pastoris* X33

The $CHMO_{Acineto}$-Mut gene was amplified using pET-28a(+)-$CHMO_{Acineto}$-Mut as the template by PCR under the following conditions: pre-denaturation at 95°C for 3 min; 29 cycles at 98°C for 10 s, 55°C for 15 s, and 72°C for 105 s; followed by a final extension at 72°C for 10 min. The primers used in this study were shown in **Table S1**. The PCR product was ligated into pPICZαA/pGAPZαA and then cloned into *E. coli* DH5α. About 5 μg plasmids were linearized by *Sac* I for 6 h and recovered with PCR purification Kit

(Aidlab Biotechnologies Co., Ltd, Beijing, China), and then electrotransformed into *P. pastoris* X33 with a Micropulser (BioRad, Hercules, CA, USA). Transformants were selected on YPD (supplemented with zeocin) plates after incubation for 48 h at 30°C.

Positive yeast transformants were cultured for 24 h in test tubes containing 4 mL of YPD medium with 100 μg/mL zeocin at 28°C and 200 rpm, and then 1 mL of the culture was inoculated into 100 mL of BMGY medium containing 100 μg/mL ampicillin. After cultivation at 28°C, 200 rpm until optical density of the yeast cells arrived at 1–2, cells were resuspended in BMMY medium and further induced at 28°C, 200 rpm for 96 h. Neat methanol (1%, v/v) was added into the medium at further 24, 48, 72 and 96 h.

Purification of CHMO$_{Acineto}$-Mut expressed in yeast

After cultivation, cells were removed from the induced yeast fermentation broth by centrifugation at 6,000×*g*, 4°C for 40 min. About 500 mL fermentation clear broth was subjected to microfiltration (0.45 μm), concentrated by ultrafiltration on a Labscale^{TM} Tangential Flow Filtration System (Merck Millipore, German) equipped with a 30 *k*Da cut off module (Pellicon® XL, 50 cm^2, Millipore, Germany). The concentrated broth was diluted and concentrated twice with Ni-NTA buffer A. Samples were centrifugated at 10,000×*g*, 4°C for 30 min to remove deactivated proteins, then further purified by Ni^{2+}-affinity chromatography (Ren et al. 2020) and flash frozen in liquid nitrogen, stored at −80°C for further analysis.

High level production of CHMO$_{Acineto}$-Mut by high cell density fermentation

CHMO$_{Acineto}$-Mut-$_P$: single recombinant yeast colony was isolated on YPDZ agar plates and pre-cultured (200 rpm, 30°C) in 200 mL liquid YPD medium which contained ampicillin (100 μg/mL) until the optical density of the cells arrived at 2.0, then inoculated into a 5-L bioreactor (BXBIO, shanghai, China) which contained 1.8 L BSM medium. The fermentation was carried out at 28°C, DO>20%, and pH 6.0. After about 18 h of the fermentation, the DO value was suddenly rebounded to 100%, indicating the consumption of glycerol in the initial medium, and then glycerol feeding was started until an OD_{600} of about 200. A starvation was kept for 1 h to make sure the metabolism intermediates of glycerol were consumed. Then methanol induction was started with an initial rate of 4 mL/h during the first 4 h to make the yeast adapt to methanol before being stepped to a higher rate of about 18 mL/h in 12 h. After the fermentation, cells were removed and the yeast secretion supernatant was kept on ice for further analysis.

CHMO$_{Acineto}$-Mut-$_E$: single recombinant *E. coli* colony was isolated on LBK agar plates and precultured (180 rpm, 37°C) in 300 mL liquid bacterial fermentation medium supplied with kanamycin (50 μg/mL) in shake flask until the optical density arrived at 1.5, then inoculated into 5-L bioreactor which contained 2.7 L bacterial fermentation medium. The fermentation was carried out at 37°C, DO>20%, and pH 7.0. After 4 h, the complexed feeding medium was supplied with a constant rate of 25 mL/h. Cells were induced

when the OD_{600} arrived about 8.0 by adding IPTG stock solution to a final concentration of 200 μM at 25°C.

Protein assays and determination of the FAD occupation rate

The concentration of $CHMO_{Acineto}$-Mut was determined by Bradford method, using bovine serum albumin (BSA) as the standard. UV-vis scanning was performed on a Molecular Devices SpectraMax M2 Microplate Reader (USA). Determination of FAD occupation was modified from Fraaije's work [Fraaije et al. 2005], purified $CHMO_{Acineto}$-Mut samples were diluted to 5 mg/mL by denature buffer (potassium phosphate, 20 mM, pH 8.0; NaCl, 150 mM; DTT, 1 mM; SDS, 1%, w/v) and incubated at 95°C for 5 min, then the absorbance was analyzed in the wavelength range of 280-447 nm, respectively.

Determination of intracellular FAD content of *E. coli* and *P. pastoris*

At the scheduled time, cells (*E. coli* or *P. pastoris*, 132 OD) were resuspended in 100 mM potassium phosphate buffer (pH 9.0, 0.5 mL), the suspension was subjected to agitation at 1500 rpm, 4°C for 30 min by 200 mg glass beads (Φ 1 mm). A clear cell lysate was obtained by centrifugation of the sample at 10,000×*g*, 5 min. Samples were further incubated at 95°C for 10 min and centrifugated again at 10,000×*g* for 10 min to remove the protein. The resultant supernatant was subjected to HPLC analysis by a SHIMADAZU LC2010A system equipped with a C18 column (250 mm × 4.6 mm, 10 μm particle size, DEAIC), under 30°C, 447 nm, using methanol/water (6/4, *v*/*v*, 0.6 mL min^{-1}) as the mobile phase (t_R FAD = 4.531 min).

Glycosylation characterization of $CHMO_{Acineto}$-Mut

Purified $CHMO_{Acineto}$-Mut-$_E$ and $CHMO_{Acineto}$-Mut-$_P$ was diluted with denature buffer to 1 mg/mL and incubated at 95°C for 10 min, then cooled to room temperature. 10 μg of the sample was mixed with 10 μg of the *Sp*Endo H and incubated at 37°C for 1 h. Expression, purification of *Sp*Endo H was conducted according to our previous work [Zheng et al. 2020]. Samples were further analysed by SDS-PAGE.

Bio-asymmetric oxidation of pyrmetazole

After cultivation, cells were removed by centrifugation at 6,000×*g*, 4°C for 30 min. The pH value of the resulting fermentation clear broth was adjusted to 8.0 by slowly dropping 1 M K_2CO_3 aqueous solution at 0°C. For 10-mL scale reactions, the reactions were performed in closed 50 mL shake flask which contained 100 mM potassium phosphate buffer (pH 8.0), 0.2 mM $NADP^+$, lyophilized *Bst*FDH preparation. The reaction was initiated by adding 1 mL pyrmetazole methanol stock solution and shaken at 25°C, 180 rpm. For 0.6 L scale bio-oxidation reaction, the reaction was performed in a jacked 1 L fermenter, and the reaction mixture was scaled up. At the schedule time, 100 μL of the reaction mixture was taken, extracted by ethyl acetate (0.5 mL) and analyzed by chiral HPLC [Xu et al., 2020].

Purification and characterization of esomeprazole sodium salt

Purification of the esomeprazole sodium was conducted according to the modified procedure by Xu et al [Xu et al., 2020]. After the reaction was finished, the pH was adjusted to 11 by NaOH and subjected to centrifugation at 6000×*g* for 0.5 h. The supernatant was neutralized by acetic acid to pH 7, then extracted by ethyl acetate. The combined organic layers were dried over anhydrous Na_2SO_4, concentrated under reduced pressure. The resultant residual was dissolved in ethanol, added with 1 equiv. of NaOH powers, and the resulting solution was crystalized in cold ethanol/methyl-tert-butyl-ester to afford esomeprazole sodium salt.

Results And Discussion

Construction of recombinant *P. pastoris* for secretory expression of CHMO$_{Acineto}$-Mut

First, expression of CHMO$_{Acineto}$-Mut under the control of the strong, tightly regulated *AOX*1 promoter and the constitutive *GAP* promoter was compared. To do this, the gene encoding CHMO$_{Acineto}$-Mut [Bong et al. 2014] was ligated into pPICZαA and pGAPZαA. Next, the expression cassettes were integrated into the *P. pastoris* X33 (His^+, Mut^+) genome via transformation of the linearized plasmids and subsequent homologous recombination. Zeocin-resistant transformants were selected and rescreened by incubating cultures in shake flasks and testing the culture supernatants for pyrmetazole oxidation activity. The fermentation activity of the X33-pGAPZαA-CHMO$_{Acineto}$-Mut strains peaked at 10 U/L, even when glucose was supplied (**Figure 1A**). In contrast, an approximately 65-*k*Da protein band increased in intensity in parallel with increasing pyrmetazole oxidation activity (from 12 to 41 U/L) when CHMO$_{Acineto}$-Mut was expressed under the control of the *AOX*1 promoter (**Figure 1B**). Therefore, we selected this strain for further investigation. To identify strains with multiple integration events, X33-pPICZαA-CHMO$_{Acineto}$-Mut transformants were grown on YPDZ plates with different zeocin concentrations. The strain that exhibited the greatest zeocin resistance (**Figure S1**) and the highest CHMO production was selected for use in all subsequent experiments.

Characterization of the activity of CHMO$_{Acineto}$-Mut expressed by different microbial hosts

To characterize the activity of recombinant CHMO$_{Acineto}$-Mut secreted by *P. pastoris*, we constructed a *P. pastoris* strain expressing CHMO$_{Acineto}$-Mut with a *C*-terminal histidine tag. The tagged CHMO$_{Acineto}$-Mut was then purified from the yeast supernatant by ultrafiltration followed by Ni-NTA chromatography. Surprisingly, CHMO$_{Acineto}$-Mut expressed by yeast (CHMO$_{Acineto}$-Mut-$_P$) exhibited approximately 4 times greater specific activity than CHMO$_{Acineto}$-Mut expressed by *E. coli* (CHMO$_{Acineto}$-Mut-$_E$). Next, we determined the Michaelis-Menten kinetic constants of pyrmetazole oxidation by CHMO$_{Acineto}$-Mut-$_P$ and CHMO$_{Acineto}$-Mut-$_E$ (**Table 1**) to investigate biochemical differences in CHMO$_{Acineto}$-Mut expressed by different hosts. There was no difference between CHMO$_{Acineto}$-Mut-$_P$ and CHMO$_{Acineto}$-Mut-$_E$ in terms of affinity for pyrmetazole; however, CHMO$_{Acineto}$-Mut-$_P$ exhibited a 3.2-fold higher turnover frequency (k_{cat}) than CHMO$_{Acineto}$-Mut-$_E$. Similar phenomenon was observed in the kinetic profiles of NADPH, indicating that CHMO$_{Acineto}$-Mut-$_P$ has greater catalytic efficiency than CHMO$_{Acineto}$-Mut-$_E$.

In parallel, we noted that CHMO$_{Acineto}$-Mut-$_P$ showed more intense yellow color during the purification process, albeit when it was diluted to the same protein concentration of CHMO$_{Acineto}$-Mut-$_E$. Because this enzyme belongs to the type I BVMO superfamily, it is functionally dependent on flavin adenine dinucleotide (FAD), which is the source of the yellow color of the enzyme. We determined the UV-visual spectrum profile of CHMO$_{Acineto}$-Mut-$_P$ and CHMO$_{Acineto}$-Mut-$_E$ at a concentration of 5 mg/mL. As expected, the characteristic twin peaks of isoalloxazine (FAD) in CHMO$_{Acineto}$-Mut-$_P$ were significantly higher than those of CHMO$_{Acineto}$-Mut-$_E$, indicating higher FAD occupation (**Figure 2A**). Given that FAD absorbs light at a wavelength of 447 nm [Fraaije et al. 2005], we determined the A_{280}/A_{447} of the two denatured CHMOs and found that CHMO$_{Acineto}$-Mut-$_P$ had about 3.5-fold higher FAD occupation than CHMO$_{Acineto}$-Mut-$_E$ (**Figure 2B**), which is in consist with the higher k_{cat} value of CHMO$_{Acineto}$-Mut-$_P$ than CHMO$_{Acineto}$-Mut-$_E$.

Next, we added different amounts of free FAD to the activity determination system to determine whether it affected the activity of the heterologously expressed proteins. As expected, a stepwise increase in enzyme activity (up to about 1.5-fold, **Figure 2C**) that correlated with increasing FAD concentrations was observed for CHMO$_{Acineto}$-Mut-$_E$ but not CHMO$_{Acineto}$-Mut-$_P$. Interestingly, during the induction phase of fermentation, yeast contained more intracellular FAD than *E. coli* (**Figure 2D**), which indicates that using yeast as the expression host results in a greater FAD supply, as well as greater incorporation of FAD into the recombinant CHMO$_{Acineto}$-Mut. These results demonstrated that the eukaryotic *P. pastoris* is a better system for expressing FAD-dependent enzymes than the prokaryotic *E. coli*.

Next, we assessed *N*-glycosylation of CHMO$_{Acineto}$-Mut-$_P$ by digesting with *Streptomyces plicatus* endoglycosidase H (**Figure S3**). The results confirmed that *N*-glycosylation of CHMO$_{Acineto}$-Mut-$_P$ occurred only at the *N*-glycosylation motif (N-X-T/S) at Asn249. However, glycosylation did not change the thermostability of CHMO$_{Acineto}$-Mut. Furthermore, the T_m values for CHMO$_{Acineto}$-Mut-$_P$ and CHMO$_{Acineto}$-Mut-$_E$ were both 60°C, as determined by the *Thermo*FAD method (**Figure S4**) [Forneris et al. 2009].

Production of CHMO$_{Acineto}$-Mut via high-density fermentation on a 5-L scale

Production of CHMO$_{Acineto}$-Mut by either recombinant *P. pastoris* or *E. coli* in a 5-L fermenter was subsequently compared. Pyrmetazole oxidation activity was observed immediately after induction with methanol in the yeast fermentation process (**Figure 3A**). Enzyme production by recombinant *P. pastoris* peaked at 1728 ± 63 U/L, which is almost 2.8-fold that seen with recombinant *E. coli,* after 103 h of methanol feeding (**Figure 3C**). The specific activity of purified CHMO$_{Acineto}$-Mut-$_P$ was 0.95 ± 0.01 U/mg, which suggests that the concentration of CHMO$_{Acineto}$-Mut-$_P$ in the yeast fermentation broth was greater than 1.6 g/L. The high extracellular expression level of CHMO$_{Acineto}$-Mut-$_P$ was also confirmed by 10% SDS-PAGE analysis (**Figure 3B**). The most intense protein band at about 75 *k*Da represented CHMO$_{Acineto}$-Mut-$_P$, whereas the content of other proteins in the supernatant was negligible. SDS-PAGE analysis of cell-free *E. coli* extracts indicated that CHMO$_{Acineto}$-Mut-$_E$ accounted for only approximately 50% of the total

protein content (**Figure 3D**). More importantly, the cost of the raw materials needed for $CHMO_{Acineto}$-Mut-$_P$ production was less than 20% of that need to produce $CHMO_{Acineto}$-Mut-$_E$ (**Table 2**). This was primarily due to the markedly simpler growth medium composition, and further emphasizes the technical and economic advantages of employing *P. pastoris* in the production of $CHMO_{Acineto}$-Mut.

Asymmetric bio-oxidation of pyrmetazole by employing yeast secretion

One of the most important advantages of using methylotrophic yeast as an expression system for biotransformation is the direct use of yeast secretion as the catalyst [Zheng et al. 2020; Qian et al. 2014]. Bio-asymmetric synthesis of (*S*)-omeprazole by utilizing $CHMO_{Acineto}$-Mut-$_P$ in the yeast secretion was then conducted. The *Burkholderia stabilis* 15516 formate dehydrogenase gene (*Bst*FDH) [Xu et al. 2020; Hatrongjit et al. 2010] was coupled for the regeneration of the cofactor NADPH. In the initial set of experiments, moderate rates (65%–86%) of pyrmetazole conversion were observed within 17 h (**Table 3**, **entries 1 & 2**). Considering the low level of soluble oxygen in aqueous solution is usually the limitation especially for the enzymatic oxidation reactions. The reaction was then performed under an oxygen atmosphere with an oxygen balloon to supply oxygen. As expected, when additional oxygen was provided, 10 g/L of substrate was completely transformed into the target product sulfoxide (**Table 3**, **entry 3**). Based on the optimal conditions determined using a 10-mL shaker flask, the bio-asymmetric sulfoxidation reaction was scaled up to 0.6 L (**Table 3**, **entry 4**, also see **Figure S7**). After 26 h, near-complete oxidation (97% conv.) was achieved, with excellent optical purity (>99% *ee*). During extraction of the sulfoxide product from the aqueous phase, we noted that there was a remarkable decrease in $CHMO_{Acineto}$-Mut-$_P$ emulsion compared with the $CHMO_{Acineto}$-Mut-$_E$ crude extract (**Figure S6**), which we attributed to the lower concentrations of endogenous protein and nucleic acids in the yeast supernatants. Ultimately, we achieved a 73% isolation yield for the crude product, which can be refined further for pure esomeprazole sodium salt.

Conclusions

In summary, in this study we demonstrated for the first time extracellular production of $CHMO_{Acineto}$-Mut (a type I BVMO), with excellent yield and good purity, using a *P. pastoris* X33 Mut^+ expression system. When the neutralized yeast supernatants were used directly to catalyze asymmetric Kagan–Sharpless–Pitchen sulfoxidation of 10 g/L pyrmetazole, a satisfactory product *ee* and conversion rate were achieved. Moreover, using this *P. pastoris* expression system obviated two major hurdles associated with CHMO in *E. coli,* namely the insufficient FAD supply and the need for a tedious cell-disruption step. As flavin-dependent enzymes are widely used in the pharmaceutical, agricultural, food production, and synthetic chemistry industries [Baker Dockrey et al. 2019], *P. pastoris* may be a suitable host for the production of flavin-dependent enzymes for a wide range of industrial purposes. Thus, this work provides a valuable example of how efficient extracellular production of flavin-dependent biocatalysts can be achieved.

Abbreviations

*AOX*1: alcohol oxidase 1 promoter; *Bst*FDH: formate dehydrogenase from *Burkholderia stabilis* 15516; BVMO: Bayer-Villiger monooxygenase; CHMO: cyclohexanone monooxygenase; $CHMO_{Acineto}$: cyclohexanone monooxygenase from *Acinetobacter* sp. strain NCIMB 9871; $CHMO_{Acineto}$-Mut: engineered $CHMO_{Acineto}$; $CHMO_{Acineto}$-Mut-$_E$: engineered $CHMO_{Acineto}$ expressed in *E. coli* BL21 (DE3); $CHMO_{Acineto}$-Mut-$_P$: engineered $CHMO_{Acineto}$ expressed in *P. pastoris* X33; FAD: flavin adenine dinucleotide; *GAP*: Glyceraldehyde–3-phosphate dehydrogenase promoter; NAD(P)H: nicotinamide adenine dinucleotide (phosphate).

Declarations

Acknowledgement

The authors are appreciated to prof. Li-Ming Liu (Jiangnan University) for his kind providing of the *P. pastoris* strains. The authors are grateful for Miss Yin-Qi Wu (ECUST), Mr. Shi-Miao Ren (ECUST), Mr. Jun Zhu (ECUST) and Mr. Chao Shou (ECUST) for their fruitful experimental suggestions as well as experimental assistance.

Authors' contributions

YJL performed the experiments and analyzed the data; Prof. HLY and prof. JHX conceived the project; Dr. YCZ designed the experiments and wrote this paper; GQ, FL assisted the fermentation experiments; Prof. HLY, associate Prof. ZJZ and prof. JHX helped to improve the paper; and all authors read and approved the final manuscript.

Funding

This work was financially supported by the National Natural Science Foundation of China (21922804)， the National Key Research and Development Program of China (2019YFA09005000), and the Fundamental Research Funds for the Central Universities (22221818014).

Availability of data and materials

All data generated or analyzed during this study are included in this article and the supplementary information file.

Ethics approval and consent to participate

Not applicable.

Consent for publication

All authors approved the consent for publishing the manuscript to bioresources and bioprocessing.

Competing interests

The authors declare that they have no competing interests.

Author details

[1] State Key Laboratory of Bioreactor Engineering, East China University of Science and Technology, Shanghai 200237, People's Republic of China. [2] Shanghai Collaborative Innovation Center for Biomanufacturing Technology, East China University of Science and Technology, Shanghai 200237, People's Republic of China.

References

1. Fürst MJLJ, Gran-Scheuch A, Aalbers FS, Fraaije MW (2019) Baeyer–Villiger monooxygenases: tunable oxidative biocatalysts. *ACS Catal* 9:11207–11241. doi: 10.1021/acscatal.9b03396.
2. Romero E, Gómez Castellanos JR, Gadda G, Fraaije MW, Mattevi A (2018) Same substrate, many reactions: oxygen activation in flavoenzymes. *Chem Rev* 118:1742–1769. doi: 10.1021/acs.chemrev.7b00650.
3. de Gonzalo G, Mihovilovic MD, Fraaije MW (2010) Recent developments in the application of Baeyer–Villiger monooxygenases as biocatalysts. *ChemBioChem* 11:2208–2231. doi: 10.1002/cbic.201000395.
4. Forney F, Markovetz A (1969) An enzyme system for aliphatic methyl ketone oxidation. *Biochem Biophys Res Commun* 37:31–38. doi.org/10.1016/0006-291X(69)90876-6.
5. Yu JM, Liu YY, Zheng YC, Li H, Zhang XY, Zheng GW, Li CX, Bai YP, Xu JH (2018) Direct access to medium-chain α,ω-dicarboxylic acids by using a Baeyer–Villiger monooxygenase of abnormal regioselectivity. *ChemBioChem* 19: 2049–2054. doi: 10.1002/cbic.201800318.
6. Fiorentini F, Romero E, Fraaije MW, Faber K, Hall M, Mattevi A (2017) Baeyer–Villiger monooxygenase FMO5 as entry point in drug metabolism. *ACS Chem Biol* 12:2379–2387. doi: 10.1021/acschembio.7b00470.
7. van Beek HL, de Gonzalo G, Fraaije MW (2012) Blending Baeyer–Villiger monooxygenases: using a robust BVMO as a scaffold for creating chimeric enzymes with novel catalytic properties. *Chem Commun* 48:3288–3290. doi.org/10.1039/C2CC17656D.
8. Fraaije MW, Wu J, Heuts DP, van Hellemond EW, Spelberg JH, Janssen DB (2005) Discovery of a thermostable Baeyer–Villiger monooxygenase by genome mining. *Appl Microbiol Biotechnol* 66:393–400. doi: 10.1007/s00253-004-1749-5.
9. Ferroni FM, Tolmie C, Smit MS, Opperman DJ (2017) Alkyl formate ester synthesis by a fungal Baeyer–Villiger monooxygenase. *ChemBioChem* 18:515–517. doi.org/10.1002/cbic.201600684.
10. Bisagni S, Summers B, Kara S, Hatti-Kaul R, Grogan G, Mamo G, Hollmann F (2014) Exploring the substrate specificity and enantioselectivity of a Baeyer–Villiger monooxygenase from *Dietzia* sp. D5:

oxidation of sulfides and aldehydes. *Top Catal* 57:366–375. doi.org/10.1007/s11244-013-0192-1.

11. Colonna S, Gaggero N, Carrea G, Ottolina G, Pasta P, Zambianchi F (2002) First asymmetric epoxidation catalysed by cyclohexanone monooxygenase. *Tetrahedron Lett* 43:1797–1799. doi.org/10.1016/S0040-4039(02)00029-1.
12. Rial DV, Bianchi DA, Kapitanova P, Lengar A, van Beilen J, Mihovilovic M (2008) Stereoselective desymmetrizations by recombinant whole cells expressing the Baeyer–Villiger monooxygenase from *Xanthobacter* sp. ZL5: a new biocatalyst accepting structurally demanding substrate. *Eur J Org Chem* 2008:1203–1213. doi.org/10.1002/ejoc.200700872.
13. Branchaud BP, Walsh CT (1985) Functional group diversity in enzymic oxygenation reactions catalyzed by bacterial flavin-containing cyclohexanone oxygenase. *J Am Chem Soc* 107:2153–2161. doi.org/10.1021/ja00293a054.
14. de Gonzalo G, Fürst MJLJ, Fraaije MW (2017) Polycyclic ketone monooxygenase (PockeMO): a robust biocatalyst for the synthesis of optically active sulfoxides. *Catalysts* 7:288. doi.org/10.3390/catal7100288.
15. Mordhorst M, Andexer JN (2020) Round, round we go – strategies for enzymatic cofactor regeneration. *Nat Prod Rep* 37:1316–1333. doi.org/10.1039/D0NP00004C.
16. Donoghue NA, Norris DB, Trudgill PW (1976) The purification and properties of cyclohexanone oxygenase from *Nocardia globerula* CL1 and *Acinetobacter* NCIB 9871. *Eur J Biochem* 63:175–192. doi.org/10.1111/j.1432-1033.1976.tb10220.x.
17. Light DR, Waxman DJ, Walsh C (1982) Studies on the chirality of sulfoxidation catalyzed by bacterial flavoenzyme cyclohexanone monooxygenase and hog liver FAD-containing monooxygenase. *Biochemistry* 21:2490–2498. doi.org/10.1021/bi00539a031.
18. Carreno MC (1995) Applications of sulfoxides to asymmetric synthesis of biologically active compounds. *Chem Rev* 95:1717–1760. doi.org/10.1021/cr00038a002.
19. Matsui T, Dekishima Y, Ueda M (2014) Biotechnological production of chiral organic sulfoxides: current state and perspectives. *Appl Microbiol Biotechnol* 98:7699–7706. doi: 10.1007/s00253-014-5932-z.
20. Liu F, Shou C, Geng Q, Zhao C, Xu JH, Yu HL (2021) A Baeyer-Villiger monooxygenase from *Cupriavidus basilensis* catalyzes asymmetric synthesis of (*R*)-lansoprazole and other pharmaco-sulfoxides. *Appl Microbiol Biotechnol* 105:3169–3180. doi.org/10.1007/s00253-021-11230-0.
21. Zhang Y, Liu F, Xu N, Wu YQ, Zheng YC, Zhao Q, Lin GQ, Yu HL, Xu JH (2018) Discovery of two native Baeyer-Villiger monooxygenases for asymmetric synthesis of bulky chiral sulfoxides. *Appl Environ Microbiol* 84:e00638–18. doi: 10.1128/AEM.00638-18.
22. Bong YK, Song S, Nazor J, Michael V, Widegren M, Smith D, Collier SJ, Wilson R, Palanivel SM, Narayanaswamy K, Mijts B, Clay MD, Fong R, Colbeck J, Appaswami A, Muley S, Zhu J, Zhang X, Liang J, Entwistle D (2018) Baeyer–Villiger monooxygenase-mediated synthesis of esomeprazole as an alternative for Kagan sulfoxidation. *J Org Chem* 83:7453–7458. doi: 10.1021/acs.joc.8b00468.

23. Zhang Y, Wu YQ, Xu N, Zhao Q, Yu HL, Xu JH (2019) Engineering of cyclohexanone monooxygenase for the enantioselective synthesis of (*S*)-omeprazole. *ACS Sustainable Chem Eng* 7:7218–7226. doi: 10.1021/acssuschemeng.9b00224.
24. Ren SM, Liu F, Wu YQ, Chen Q, Zhang ZJ, Yu HL, Xu JH (2020) Identification two key residues at the intersection of domains of a thioether monooxygenase for improving its sulfoxidation performance. *Biotechnol Bioeng* 118:737–744. doi.org/10.1002/bit.27604.
25. Zhao P, Ren SM, Liu F, Zheng YC, Xu N, Pan J, Yu HL, Xu JH (2021) Protein engineering of thioether monooxygenase to improve its thermostability for enzymatic synthesis of chiral sulfoxide. *Mol Catal.* 509: 11625. doi.org/10.1016/j.mcat.2021.111625.
26. Hasegawa T, Takagi K, Kitaichi K (1999) Effects of bacterial endotoxin on drug pharmacokinetics. *Nagoya J Med Sci* 62:11–28.
27. Yang KH, Lee MG (2008) Effects of endotoxin derived from *Escherichia coli* lipopolysaccharide on the pharmacokinetics of drugs. *Arch Pharm Res* 31:1073–1086. doi: 10.1007/s12272-001-1272-8.
28. Chen G, Kayser MM, Mihovilovic MD, Mrstik ME, Martinez CA, Stewart JD (1999) Asymmetric oxidations at sulfur catalyzed by engineered strains that overexpress cyclohexanone monooxygenase. *New J Chem* 23:827–832. doi.org/10.1039/A902283J.
29. Stewart JD, Reed KW, Kayser MW (1996) 'Designer yeast': a new reagent for enantioselective Baeyer–Villiger oxidations. *J Chem Soc Perkin Trans* 1:755–757. doi.org/10.1039/P19960000755.
30. Karbalaei M, Rezaee SA, Farsiani H. (2020) *Pichia pastoris*: A highly successful expression system for optimal synthesis of heterologous proteins. *J Cell Physiol* 235:5867–5881. doi: 10.1002/jcp.29583.
31. Cereghino JL, Cregg JM (2000) Heterologous protein expression in the methylotrophic yeast *Pichia pastoris*. *FEMS Microbiol Rev* 24:45–66. doi: 10.1111/j.1574-6976.2000.tb00532.x.
32. Zheng YC, Li FL, Lin Z, Lin GQ, Hong R, Yu HL, Xu JH (2020) Structure-guided tuning of a hydroxynitrile lyase to accept rigid pharmaco aldehydes. *ACS Catal* 10:5757–5763. dx.doi.org/10.1021/acscatal.0c01103.
33. Bradford MM (1976) A rapid and sensitive method for the quantitation of microgram quantities of protein utilizing the principle of protein-dye binding. *Anal Biochem* 72:248–254. doi.org/10.1016/0003-2697(76)90527-3.
34. Xu N, Zhu J, Wu YQ, Zhang Y, Xia JY, Zhao Q, Lin GQ, Yu HL, Xu JH (2020) Enzymatic preparation of the chiral (*S*)-sulfoxide drug esomeprazole at pilot-scale levels. *Org Proc Res Dev* 24:1124–1130. dx.doi.org/10.1021/acs.oprd.0c00115.
35. Bong YK, Clay MD, Collier SJ, Mijts B, Vogel M, Zhang X, Zhu J, Nazor J, Smith D, Song S (2014) Synthesis of Prazole Compounds. US patent 8895271, November 25 2014.
36. Forneris F, Orru R, Bonivento D, Chiarelli LR, Mattevi A (2009) *ThermoFAD, a Thermofluor®*-adapted flavin ad hoc detection system for protein folding and ligand binding. *FEBS J* 276:2833–2840. doi.org/10.1111/j.1742-4658.2009.07006.x.

37. Qian XL, Pan J, Shen ND, Ju X, Zhang J, Xu JH (2014) Efficient production of ethyl (*R*)-2-hydroxy-4-phenylbutyrate using an economically competitive reductase expressed in *Pichia pastoris*. *Biochem Eng J* 91:72–77. dx.doi.org/10.1016/j.bej.2014.07.008.

38. Hatrongjit R, Packdibamrung K (2010) A novel $NADP^+$-dependent formate dehydrogenase from *Burkholderia stabilis* 15516: screening, purification and characterization. *Enzyme Microb Technol* 46:557–561. doi.org/10.1016/j.enzmictec.2010.03.002.

39. Baker Dockrey SA, Narayan ARH (2019) Flavin-dependent biocatalysts in synthesis. *Tetrahedron*, 75:1115–1121. doi: 10.1016/j.tet.2019.01.008

Tables

Table 1. Kinetic profiles of recombinant $CHMO_{Acineto}$-Mut expressed in *E. coli* and *P. pastoris* in pyrmetazole oxidation reactions.

Enzyme	Pyrmetazole[a]			NADPH[b]		
	K_M (mM)	k_{cat} (s^{-1})	k_{cat}/K_M (s^{-1} mM^{-1})	K_M (mM)	k_{cat} (s^{-1})	k_{cat}/K_M (s^{-1} mM^{-1})
$CHMO_{Acineto}$-Mut-$_E$	0.028 ± 0.004	0.35 ± 0.02	12.5	(11.2 ± 2.5)×10^{-4}	0.34 ± 0.02	304
$CHMO_{Acineto}$-Mut-$_P$	0.026 ± 0.001	1.12 ± 0.04	43.4	(7.1 ± 1.1)×10^{-4}	0.82 ± 0.02	1154

[a] Kinetic parameters were determined in 0.5 mL reaction scale which contained potassium phosphate (100 mM, pH 9.0), methanol (2%, *v*/*v*), various concentrations of pyrmetazole (2–400 μM), NADPH (200 μM) and appropriate amount of $CHMO_{Acineto}$-Mut. [b] Reactions were determined by employing pyrmetazole (200 μM) and various concentrations of NADPH (5–200 μM). For detailed analytical conditions, see experimental sections.

Table 2. Comparison of $CHMO_{Acineto}$-Mut production in *E. coli* and *P. pastoris*.

Strain	Fermentation time (h)	Peak activity (U/L)	Productivity ($U\ L^{-1}\ h^{-1}$)	CHMO constitution (%)	Cell disruption	Cost[a] (CNY/kU)
P. pastoris X33	119 (103)[b]	1728 ± 63	14.5	85%	N	0.66
E. coli BL21 (DE3)	19 (12)[b]	622 ± 22	32.7	50%	Y	3.44

[a] For calculation details of the cost for fermentation and preparation of $CHMO_{Acineto}$-Mut from different host, see **Table S2**. [b] Induction time.

Due to technical limitations, table 3 is only available as a download in the Supplemental Files section.

Figures

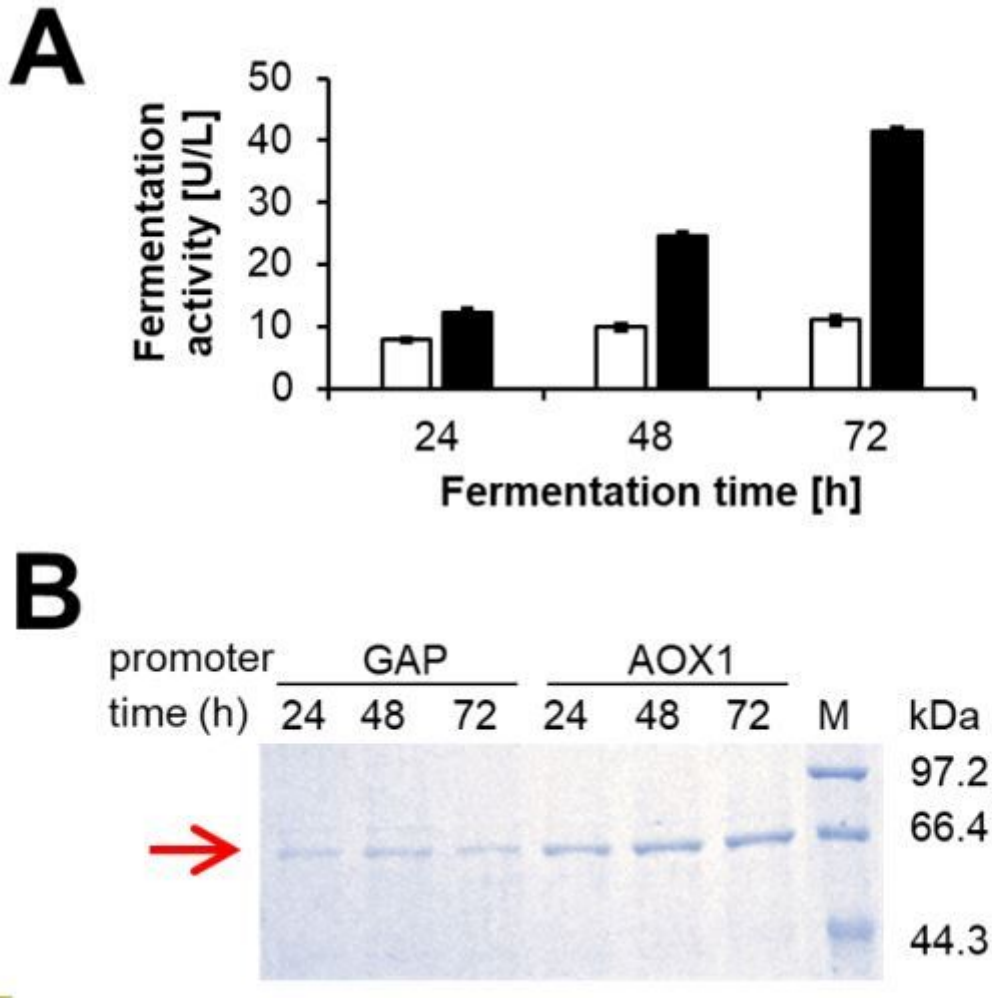

Figure 1

Initial assessment for the best CHMOAcineto-Mut extracellular production in shake flask fermentations. (A) Fermentation activity of CHMOAcineto-Mut under AOX1 promoter (■) and GAP promoter (□) with different fermentation time. (B) SDS-PAGE analysis of the extracellular expression of CHMOAcineto-Mut by P. pastoris X33 under the control of GAP and AOX1 promoters, respectively. The red arrow indicated CHMOAcineto-Mut.

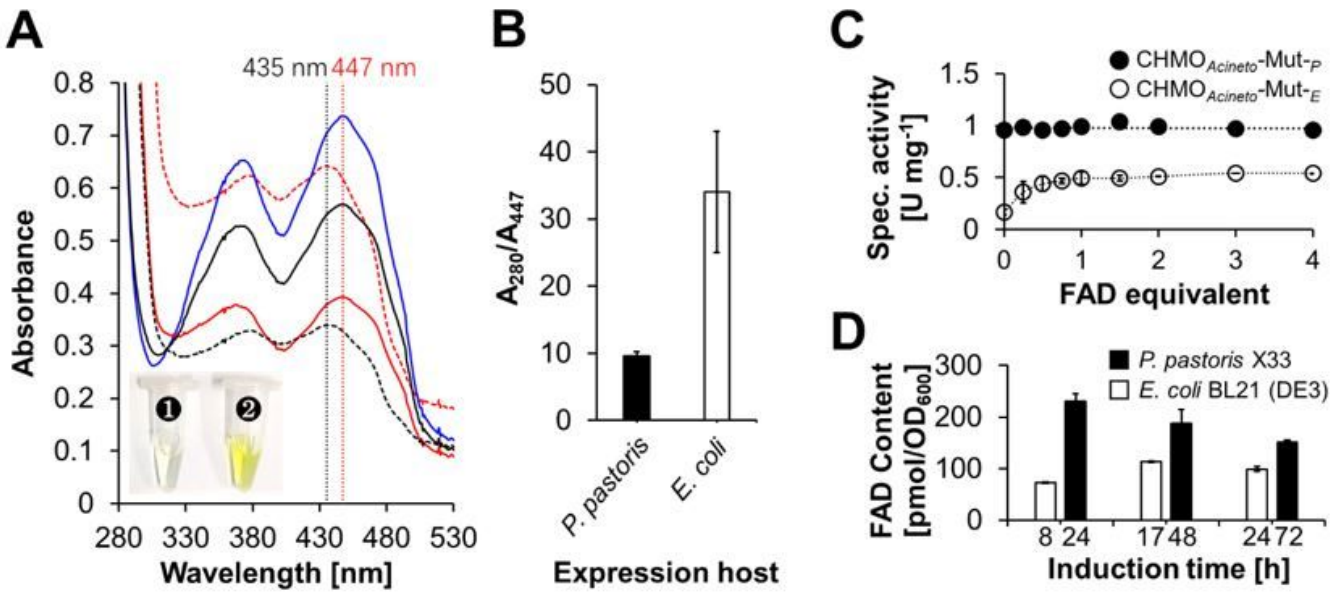

Figure 2

(A) Representative UV-visual spectrum of CHMOAcineto-Mut-P (red dash line), CHMOAcineto-Mut-E (black dash line), free FAD (blue solid line), boiled CHMOAcineto-Mut-P (black solid line) and boiled CHMOAcineto-Mut-E (red solid line); and photograph showing the color of CHMOAcineto-Mut-E (), CHMOAcineto-Mut-P () with the same concentration (5 mg/mL). (B) Calculated A280/A447 value of CHMOAcineto-Mut expressed by different hosts according to the UV-vis spectrum analysis. (C) Specific activity of CHMOAcineto-Mut-P (□) and CHMOAcineto-Mut-E (●) supplied with different amounts of free FAD. (D) Intracellular FAD constitution of P. pastoris X33 and E. coli BL21 (DE3) during the expression of CHMOAcineto-Mut.

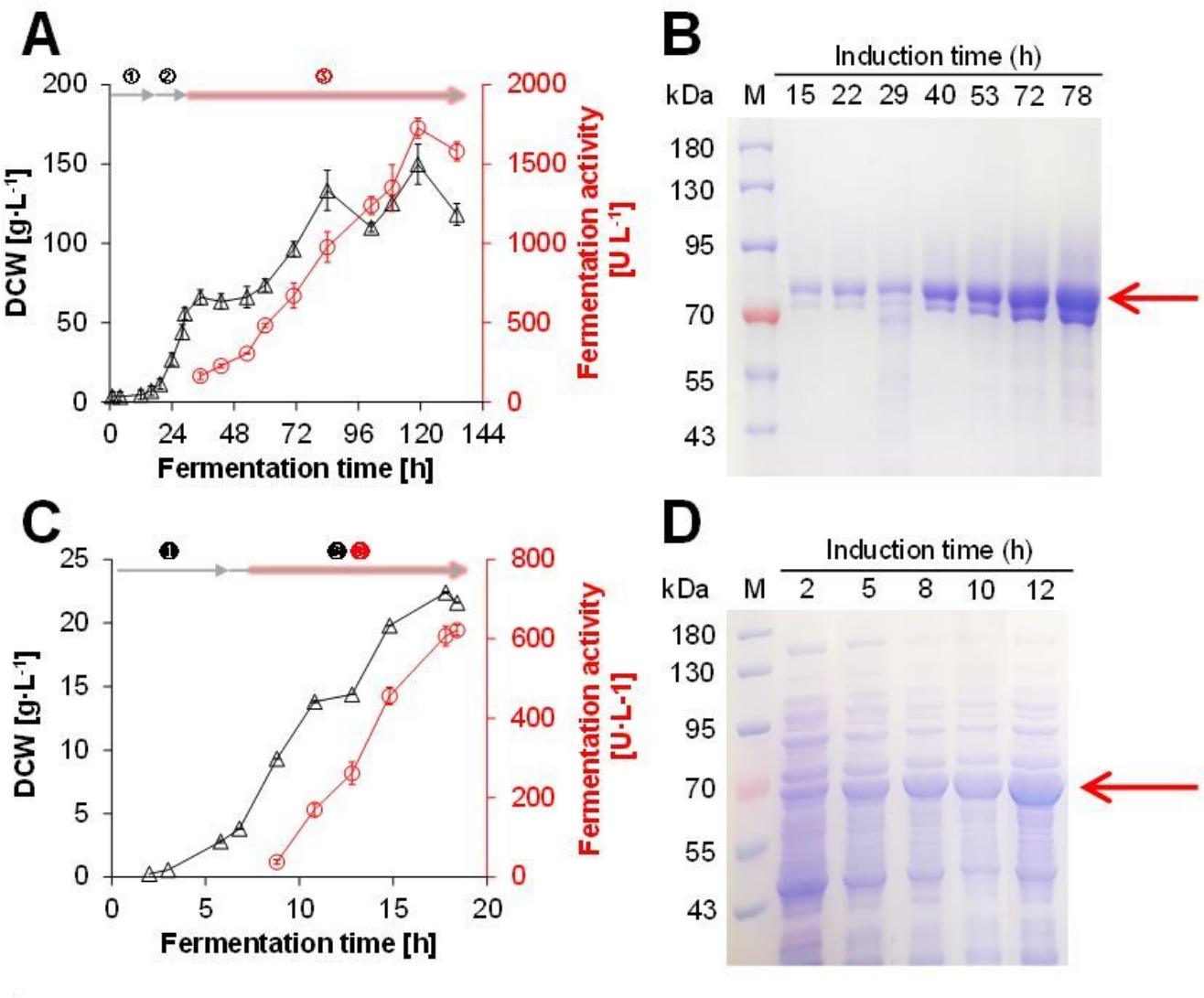

Figure 3

Time course of high-cell-density fermentation of strain X33-pPICZαA-CHMOAcineto-Mut (A) or BL21 (DE3)-pET-28(a)+-CHMOAcineto-Mut (C) in 5 L fermentator and the SDS-PAGE analysis of the yeast fermentation clear broth (B) or the cell-free extract of the E. coli (D) during the induction processes. For the P. pastoris fermentation, the time course was divided into the glycerol consumption (①), glycerol feeding (②) and methanol induction (③); and corresponding to the glycerol consumption (①), glycerol feeding (②) and IPTG induction (③) for E. coli. lane M, protein marker; the red arrow highlighted the band of CHMOAcineto-Mut.

Supplementary Files

This is a list of supplementary files associated with this preprint. Click to download.

- Graphicabstract.docx

- SI20210607ZYCR.docx
- Table3.docx